This is a preprint, the final version is subject to change, of the American Mineralogist (MSA)
Cite as Authors (Year) Title. American Mineralogist, in press.
(DOI will not work until issue is live.) DOI: http://dx.doi.org/10.2138/am.2014.4693

Revision 1

Subsolidus Isothermal Fractional Crystallization

David London

ConocoPhillips School of Geology and Geophysics

University of Oklahoma

Norman, Oklahoma USA 73019

dlondon@ou.edu

ABSTRACT

In theory, multicomponent silicate liquids of minimum or eutectic composition should crystallize their solidus phases simultaneously and in their invariant proportions. In reality, the crystallization of those liquids of granitic composition produces sequential assemblages and normal fractional crystallization of solid solutions when crystallization commences at or along an isotherm well below the solidus of the system. The sequence of mineral assemblages derives principally from their relative stabilities, as measured by the Gibbs free energy change for the reaction of melt to crystals in the metastable region below the liquidus surface, rather than chemical concentration alone. Whereas crystallization close to the solidus ($\Delta T \approx 50$ ºC) promotes the simultaneous (eutectic) crystallization of quartz and feldspars that leads to the formation of granite, large liquidus undercooling ($\Delta T \approx 200$ ºC) produces sequential assemblages from the margins to centers of melt bodies. The liquidus undercooling that drives subsolidus isothermal fractional crystallization is the single-most important process for the generation of zoned granitic pegmatites.

KEY WORDS: granite, pegmatite, liquidus undercooling, fractional crystallization, internal zonation

LIQUIDUS RELATIONSHIPS IN THE GRANITE SYSTEM

Though liquidus diagrams are utilized to model crystallization of initially crystal-free melts, all such diagrams are actually derived from thermally prograde partial melting experiments in which little or nothing crystallizes (Bowen 1928). This is because silicate liquids, and in particular viscous, high-silica liquids that correspond to the compositions of granites (*s.l.*), tend to persist metastably well below their liquidus or solidus (Fig. 1a), and hence are of little value in locating those phase boundaries upon cooling.

In the case of equilibrium crystallization, a melt of minimum or eutectic composition that cools to its solidus should crystallize quartz and alkali feldspars simultaneously in their invariant proportion. That crystallization will not take place precisely at the temperature of the minimum or eutectic because some degree of supersaturation is necessary to initiate the nucleation and continued growth of crystals. For igneous systems, the most common cause of supersaturation is cooling (Fig. 1a); undercooling of up to 50 ºC may be necessary to initiate crystallization in granitic liquids, irrespective of the rate of cooling or time at temperature (Fig. 1a). Within ~ 50-75 ºC of the solidus, however, the driving force to crystallize quartz and feldspar is nearly equivalent (Fig. 1b), and hence there is a nearly equal probability that both will crystallize simultaneously, as is the general case for granite. Pegmatites of essentially the same granitic composition are now known to begin their crystallization at ~ 450 ºC, which is 280 ºC (ΔT) below the solidus of the hydrous granite system (Ab-Or-Qtz-H_2O (Chakoumakos and Lumpkin

1992; Morgan and London 1999; Webber et al. 1999; London 2008; London et al. 2012; Colombo et al. 2012). Equilibrium theory as it has been applied to pegmatites predicts that even at large undercooling, the crystalline product should be a simultaneous eutectic assemblage (Burnham and Nekavasil 1986).

DYNAMIC CRYSTALLIZATION EXPERIMENTS

Experiments that were aimed at assessing the crystallization response of felsic and granitic liquids as functions of undercooling were termed "*dynamic crystallization*" experiments (e.g., Swanson 1977; Fenn 1977). London et al. (1989) conducted dynamic crystallization experiments with obsidian from Macusani, Peru; the composition of that obsidian is virtually identical to the Tanco rare-element pegmatite, Manitoba (Stilling et al. 2006). Melt containing 4 wt% H_2O derived from the Macusani obsidian (saturated at ~ 10 wt% H_2O) at 200 MPa was taken to its liquidus of ~ 750 ºC, then cooled isobarically to 550º-575 ºC (ΔT = 175º-200 ºC) before crystallization commenced. In all cases, the initial assemblage consists mostly of plagioclase (An_{12}) that is more calcic than the bulk composition (An_3). That calcic plagioclase (+ quartz ± zinnwaldite) evolves to albite (An_2) – K-feldspar pairs (Fig. 2); compositions of the coexisting feldspars closely match the equilibrium solvus compositions at the P and T of the experiments. With continued crystallization in the H_2O-undersaturated system, the melt fractionates toward a composition that is sodic, alkaline (in relation to measures of A/CNK or ASI), and enriched in fluxing components (B, P, and F), water (H), and rare alkalis (Li, Rb, Cs). However, that evolved melt composition first appears as a boundary layer of liquid adjacent to crystallization fronts (see Fig. 5a of London and Morgan 2012).

Dynamic crystallization involving a 200 MPa minimum haplogranite composition (normative wt% $Ab_{38.23}Or_{28.72}Qtz_{33.04}Crn_{0.01}$) with 3 wt% B_2O_3 glass and no water added at 450°C ($\Delta T \approx$ 300°C) and 200 MPa (London 1999) produced mineralogical and textural zonation that strongly resemble the alternations found in pegmatites (London 2008, London et al. 2012). Inward from the margins to center (Fig. 3), the charge contains four textural - mineralogical zones: (1) graphic quartz-feldspar intergrowth, (2) crenulate layered aplite, (3) pure feldspar surrounding (4) a central core of pure quartz. Like pegmatites (London 2008; London et al. 2012), the outer and zones of that experiment contain less quartz (normative 26 wt%) than the bulk composition; the commensurate quartz content that brings the bulk composition to the minimum composition of granite lies in the pure quartz core.

In the same minimum-melt composition at 200 MPa H_2O, crystallization at $\Delta T \approx$ 75º-100 ºC produced skeletal K-feldspar crystals only (Evensen 2001). At larger undercooling ($\Delta T \approx$ 150º-200 ºC), the same skeletal K-feldspar crystals formed first, and were overgrowth by a graphic intergrowth of quartz and more sodic feldspar. At ΔT = 250 ºC, the sequence of crystallization began with skeletal K-feldspar, followed by spherulitic quartz-plagioclase intergrowths, and finally monominerallic quartz. A simultaneous assemblage of quartz and alkali feldspar in the proportions of the minimum was not obtained in any of the undercooled experiments in this series.

SUBSOLIDUS ISOTHERMAL FRACTIONAL CRYSTALLIZATION

Parsons (1969) may have been the first to observe that isobaric-isothermal subsolidus crystallization of solid solutions from undercooled melt produces a sequential evolution of

mineral compositions that closely matches the anticipated fractionation sequence and line of descent on the liquidus. Parsons noted that the products of isothermal-isobaric crystallization may be indistinguishable from a normal liquidus fractionation trend. London (2008, p. 278-279) provided a theory to explain the behavior in the granite system. In the haplogranite system, the slopes of the liquidus surfaces for quartz and feldspars are not equivalent (Fig. 1b). Hence, their metastable extensions below the solidus diverge, to different extents, from the projection of the minimum or eutectic composition to the actual subsolidus temperature of crystallization. Along the liquidus surface, and at the minimum or euctectic, the free energy (ΔG) of the reactions $\mu_{i,L} \rightarrow \mu_{i,Xl}$, which correspond to the chemical potentials of components in melt and their equivalent crystalline phases, is zero for all, and values of ΔG become increasingly negative below the solidus. Relative to the composition and temperature of undercooling, however, $-\Delta G$ is greater for some phases than for others, and for the high-temperature ends of solid solutions. For this reason, the driving force to crystallize phases is not equivalent at a temperature well below the solidus, and the first phase to crystallize is that whose free energy change ($-\Delta G$) for the crystallization reaction is greatest. As a result, crystallization is sequential, even for minimum or eutectic liquid compositions.

Isothermal subsolidus fractional crystallization is a general consequence for any multi-component liquid that can persist metastably to temperatures well below its solidus before crystallization commences, and that can crystallize multiple phases (e.g., the haplogranite ternary system) or solid solutions (e.g., the plagioclase subsystem). As applied to pegmatites, the first phases to crystallize along the margin will be those species or solid solutions whose chemical potentials in the melt are highest at the undercooled state. Consequently, feldspars predominate

over quartz, plagioclase precedes K-feldspar, and the most calcic plagioclase and mafic minerals, with their higher actual liquidus temperatures, crystallize first -- both in experiments and in nature.

THE PEGMATITE PUZZLE

In their landmark summary, Cameron et al. (1949) stated that crystallization in pegmatites is sequential, from the margins to center, *"…as successive layers upon the walls of the chamber enclosing a body of pegmatitic liquid, and hence are due primarily to fractional crystallization"* (Cameron et al. 1949, p. 105). As evidence, they cited the unidirectional solidification texture of crystals that expanded inward from margin to core, and the normal fractionation of plagioclase from An_{12} at the margins to ~ An_2 at the center (Cameron et al. 1949, p 100). The salient features of a body of pegmatite, therefore, were reconciled to an igneous model using the principles inherent in Bowen's (1928) concepts of fractional crystallization from silicate melts.

The problem, which Jahns (Jahns and Tuttle 1963; Jahns and Burnham 1969; Jahns 1982) later sought to address, was that the compositions of pegmatites are those of the eutectic proportions of granite, in which plagioclase, K-feldspar, and quartz should crystallize simultaneously in their invariant proportions. By regarding pegmatites as granitic liquids crystallizing at equilibrium, Jahns and Burnham (1969; Jahns 1982; Burnham and Nekvasil 1986) implicitly required that the crystallization of H_2O-saturated, pegmatite-forming melts at mid-crustal pressures (~ 200-400 MPa) occurs at temperatures close to that of the hydrous granite minimum, which is in the range of 650º-685 ºC over this interval of pressure (Tuttle and Bowen 1958). The principal reason for the failure of the Jahns-Burnham model (London 2008) was its constraint of equilibrium

crystallization on the liquidus of the hydrous granite system. That constraint has been removed with recent assessments of the actual conditions at which pegmatites crystallize.

In pegmatites, sequential (rather than simultaneous) crystallization of minimum or eutectic bulk compositions, and extended fractional crystallization of feldspars, including major and minor components, can now be reconciled to the process of subsolidus isothermal fractional crystallization. Other processes, including chemical diffusion, manifested by local and far-field chemical gradients (Morgan et al. 2008; London 2009, London et al. 2012; Acosta-Vigil et al. 2012), are important as well. The salient features of pegmatites, however, can now be reproduced and explained in laboratory simulations that are appropriately scaled in P, T, bulk composition, and time through the crystallization of hydrous but not H_2O-saturated, flux-bearing but not unusual granitic melts at liquidus undercooling of ~ 200°C.

ACKNOWLEDGMENTS

Special thanks go to George Morgan for his contributions of electron imaging and chemical analysis, and to students and post-graduates whose individual research projects have contributed to this comprehensive summary. Thanks also to reviewers Al Falster, Rais Latypov, and associate editor Ian Swainson for their assistance in the final preparation of this manuscript. This research has been supported since 1986 by grants the National Science Foundation. The electron microprobe lab on which so much of this work rests was funded by the U.S. Department of Energy.

REFERENCES

Acosta-Vigil, A., London, D., and Morgan, G.B. VI (2012) Chemical diffusion of major and minor components in granitic liquids: implications for the rates of homogenization of crustal melts. Lithos 153, 308-323.

Bowen, N.L. (1928) The evolution of the igneous rocks. Princeton University Press.

Burnham, C.W., and Nekvasil, H. (1986) Equilibrium properties of granite pegmatite magmas. American Mineralogist 71, 239-263.

Cameron, E.N., Jahns, R.H., McNair, A.H., and Page, L.R. (1949) Internal structure of granitic pegmatites. Economic Geology Monograph 2, 115 p.

Chakoumakos, B.C., and Lumpkin, G.R. (1990) Pressure-temperature constraints on the crystallization of the Harding pegmatite, Taos County, New Mexico. Canadian Mineralogist 28, 287-298.

Colombo, F., Sfragulla J., and Gonzáles del Tánago, J. (2012) The garnet - phosphate buffer in peraluminous granitic magmas: a case study from pegmatites of the Pocho District, Córdoba, Argentina. Canadian Mineralogist 50, 1555-1571.

Evensen, J.M. (2001) The geochemical budget of beryllium in silicic melts & superliquidus, subliquidus, and starting state effects on the kinetics of crystallization in hydrous haplogranite melts. Unpublished Ph.D. dissertation, University of Oklahoma, Norman, Oklahoma, 293 p.

Fenn, P.M. (1977) The nucleation and growth of alkali feldspars from hydrous melts. Canadian Mineralogist 15, 135-161.

Jahns, R.H. (1982) Internal evolution of pegmatite bodies. In: Černý, P. (Ed.) Granitic Pegmatites in Science and Industry. Mineralogical Association of Canada Short Course Handbook 8, 293-327.

Jahns, R.H., and Burnham, C.W. (1969) Experimental studies of pegmatite genesis: I. A model

for the derivation and crystallization of granitic pegmatites. Economic Geology 64, 843-864.

Jahns, R.H., and Tuttle, O.F. (1963) Layered pegmatite-aplite intrusives. Mineralogical Society of America Special Paper 1, 78-92.

London, D. (1999) Melt boundary layers and the growth of pegmatitic textures. (abstr.) Canadian Mineralogist 37, 826-827.

London, D. (2008) Pegmatites. Canadian Mineralogist Special Publication 10, 368 p.

London, D. (2009) The origin of primary textures in granitic pegmatites. Canadian Mineralogist 47, 697-724.

London, D., and Morgan, G.B. VI (2012) The pegmatite puzzle. Elements 8, 263–268.

London, D., Morgan, G.B. VI, and Hervig, R.L. (1989) Vapor-undersaturated experiments in the system macusanite-H_2O at 200 MPa, and the internal differentiation of granitic pegmatites. Contributions to Mineralogy and Petrology 102, 1-17.

London, D., Morgan, G.B. VI, Paul, K.A., and Guttery, B.M. (2012) Internal evolution of a miarolitic granitic pegmatite: the Little Three Mine, Ramona, California (USA). Canadian Mineralogist 50, 1025-1054.

Morgan, G.B. VI, and London, D. (1999) Crystallization of the Little Three layered pegmatite-aplite dike, Ramona District, California. Contributions to Mineralogy and Petrology 136, 310-330.

Morgan, G.B. VI, Acosta-Vigil, A., and London, D. (2008) Diffusive equilibration between hydrous metaluminous-peraluminous liquid couples at 200 MPa (H_2O), and alkali transport in granitic liquids. Contributions to Mineralogy and Petrology, 155, 257-269.

Parsons, I. (1969) Subsolidus crystallization behaviour in the system $KAlSi_3O_8$-$NaAlSi_3O_8$-H_2O. Mineralogical Magazine, 37, 173-180.

Stilling, A., Černý, P., and Vanstone, P.J. (2006) The Tanco pegmatite at Bernic Lake, Manitoba. XVI. Zonal and bulk compositions and their petrogenetic significance. Canadian Mineralogist 44, 599-623.

Swanson, S.E. (1977) Relation of nucleation and crystal-growth to the development of granitic textures. American Mineralogist 62, 966-978.

Tuttle, O.F., and Bowen, N.L. (1958) Origin of granite in the light of experimental studies in the system $NaAlSi_3O_8$-$KAlSi_3O_8$-SiO_2-H_2O. Geological Society of America Memoir 74, 153 p.

Webber, K.L., Simmons, W.B., Falster, A.U., and Foord, E.E. (1999) Cooling rates and crystallization dynamics of shallow level pegmatite-aplite dikes, San Diego County, California. American Mineralogist 84, 708-717.

Wen, S., and Nekvasil, H. (1994) SOLVCALC. An interactive graphics program package for calculating the ternary feldspar solvus and for two-feldspar geothermometry. Computers & Geosciences, 20, 1025-1040.

FIGURES

Fig. 1. (a) Nucleation delay in the granite system for a minimum-melt composition (wt% $Ab_{38.23}Or_{28.72}Qtz_{33.04}Crn_{0.01}$) at 200 MPa H_2O. The solid parabolic curve denotes the time (t) – temperature (T) surface (at constant composition) upon which microscopic crystals appear. Dashed contours indicate the volume % of crystallization. From Evensen (2001) with additional date in London (2008). (b) T-X section through the haplogranite liquidus diagram at 200 MPa H_2O, from Tuttle and Bowen (1958), showing the relative magnitudes of free energy change for the reaction of melt to crystals ($-\Delta G$) in relation to the magnitude of liquidus undercooling.

Fig. 2. A representative experiment with Macusani glass + 3-4 wt% added H_2O, preconditioned at 750 ºC, followed by isobaric cooling to 500º-575 ºC. Graphic plagioclase + quartz along the margins radiates inward to patchy crystals of K-feldspar and albite. Isolated albite crystals occur with Li-mica and abundant quartz in the center of the charge. From London et al. (1989). (Insert) Ternary feldspar solvi at 750 ºC and 500 ºC, 200 MPa, calculated from the program SOLVCALC (Wen and Nekvasil 1994). The red dot corresponds to the normative feldspar composition of the Macusani glass. From London (2008).

Fig. 3. Backscattered electron image of experiment PEG-16, consisting of haplogranite glass ($Ab_{38.23}Or_{28.72}Qtz_{33.04}Crn_{00.01}$) with 3 wt% B_2O_3 glass and no water, which was conducted at 450 ºC ($\Delta T \approx 300$ ºC) and 200 MPa. Red arrows show the direction of crystallization inward from margins to center. From London (1999).

243 Fig. 1

244

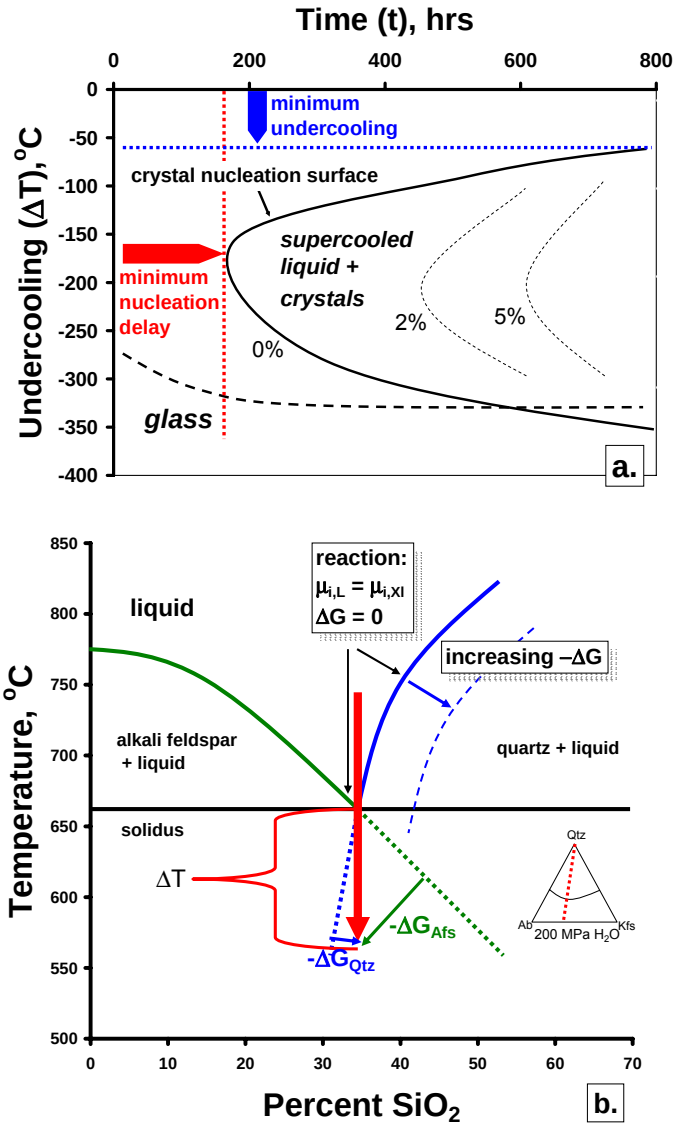

245 Fig. 2

246

247

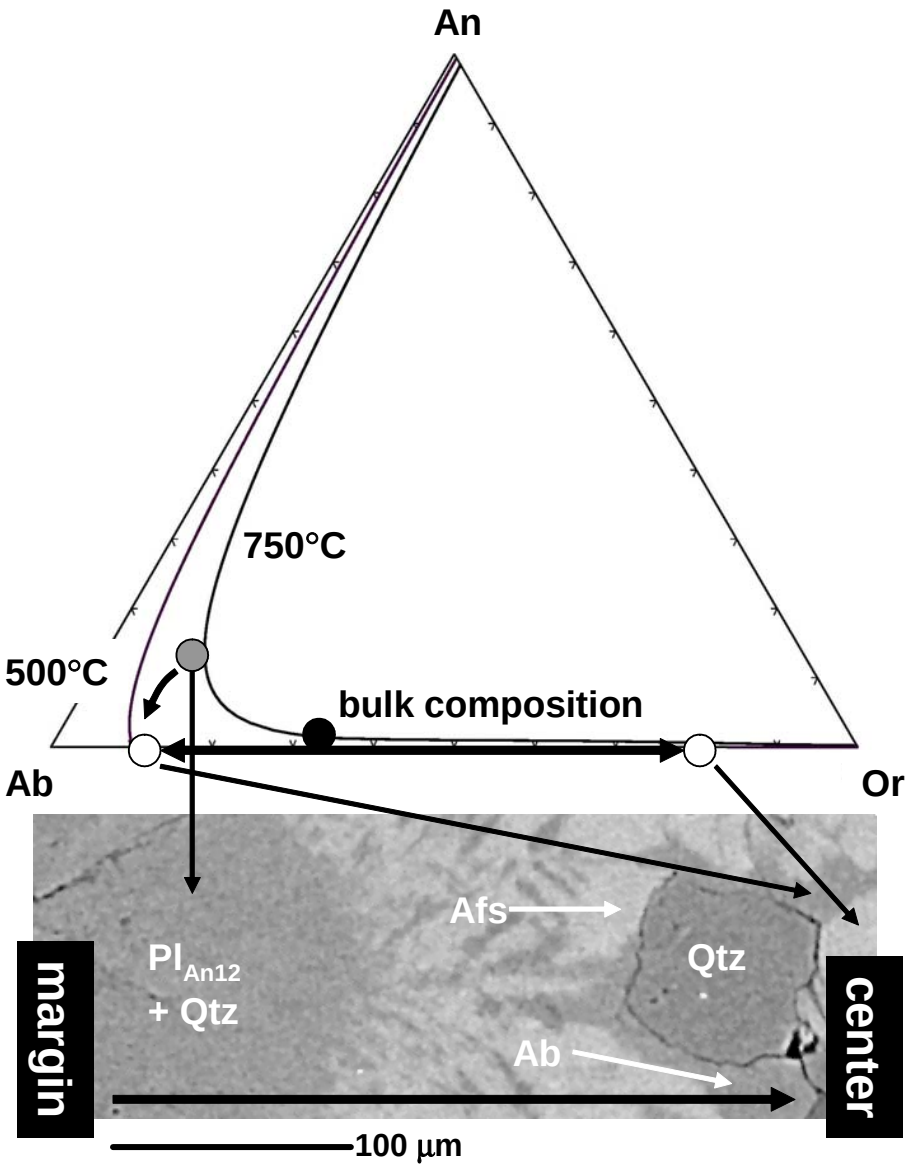

Revision 1

248 Fig. 3

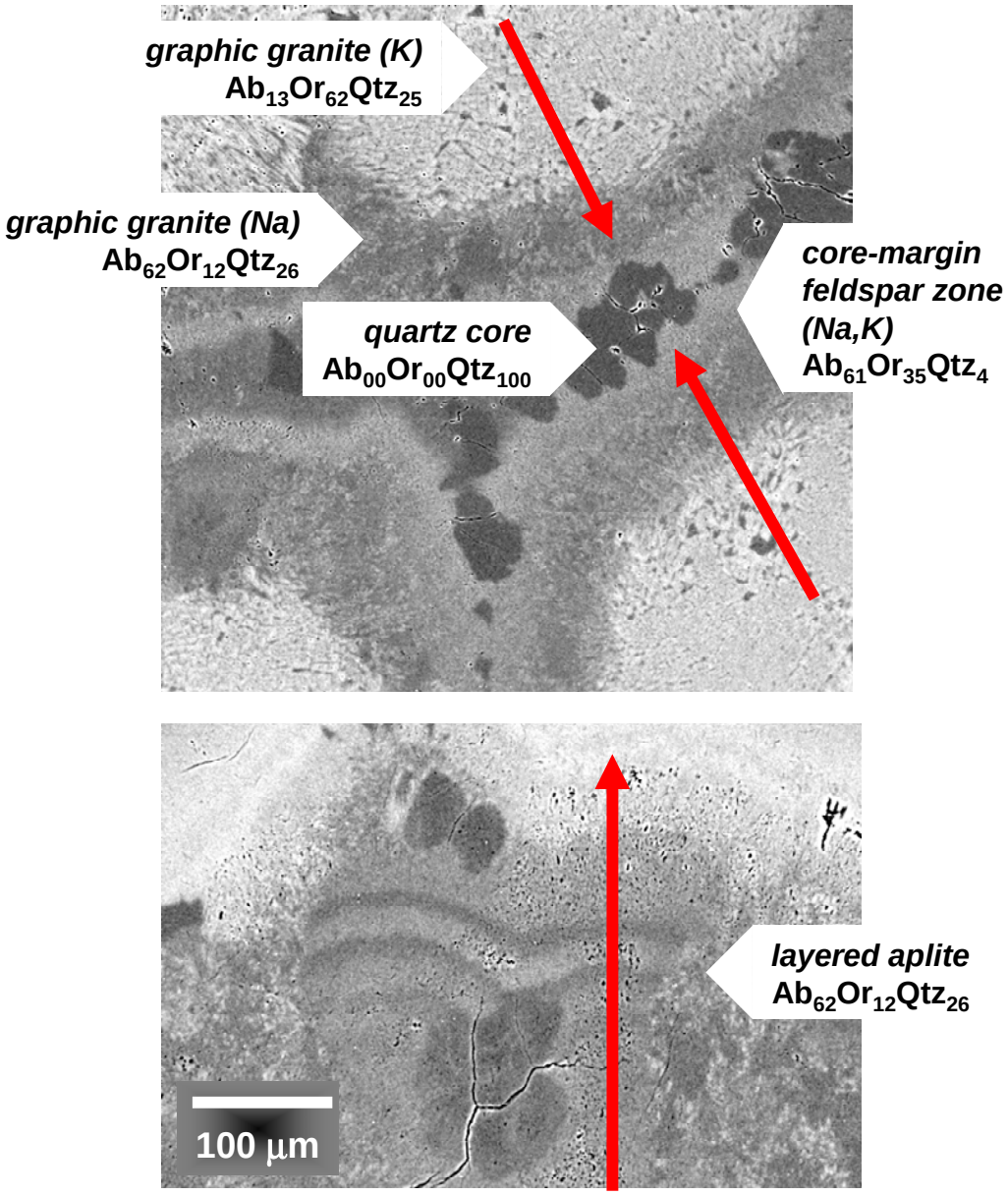

Fig 1a

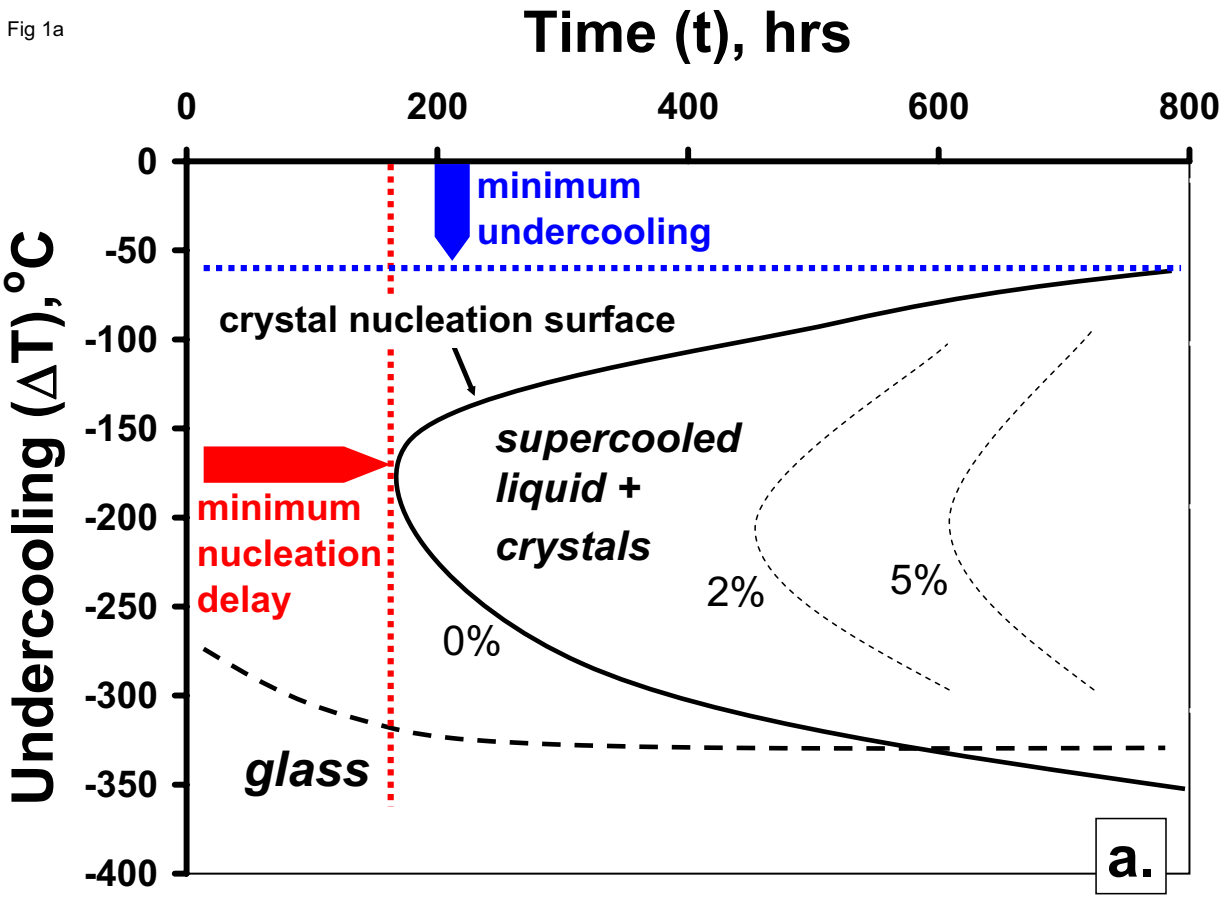
Time (t), hrs
0
200
400
600
800
0
-50
-100
-150
-200
-250
-300
-350
-400
Undercooling (ΔT), °C
minimum
undercooling
crystal nucleation surface
supercooled
liquid +
crystals
minimum
nucleation
delay
2%
5%
0%
glass
a.

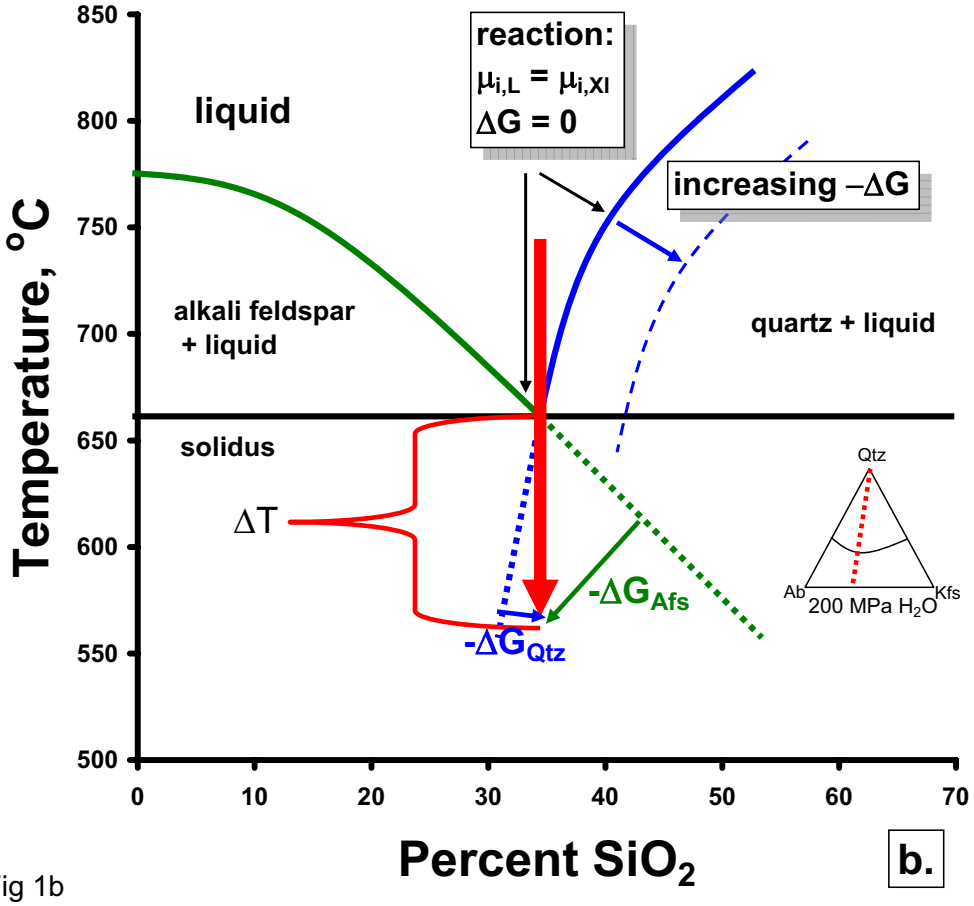
reaction:
$\mu_{i,L} = \mu_{i,xl}$
$\Delta G = 0$
liquid
increasing $-\Delta G$
alkali feldspar
+ liquid
quartz + liquid
solidus
ΔT
$-\Delta G_{Afs}$
$-\Delta G_{Qtz}$
Qtz
Ab
Kfs
200 MPa H_2O
Temperature, °C
Percent SiO_2
850
800
750
700
650
600
550
500
0
10
20
30
40
50
60
70
b.

Fig 1b

Fig. 2

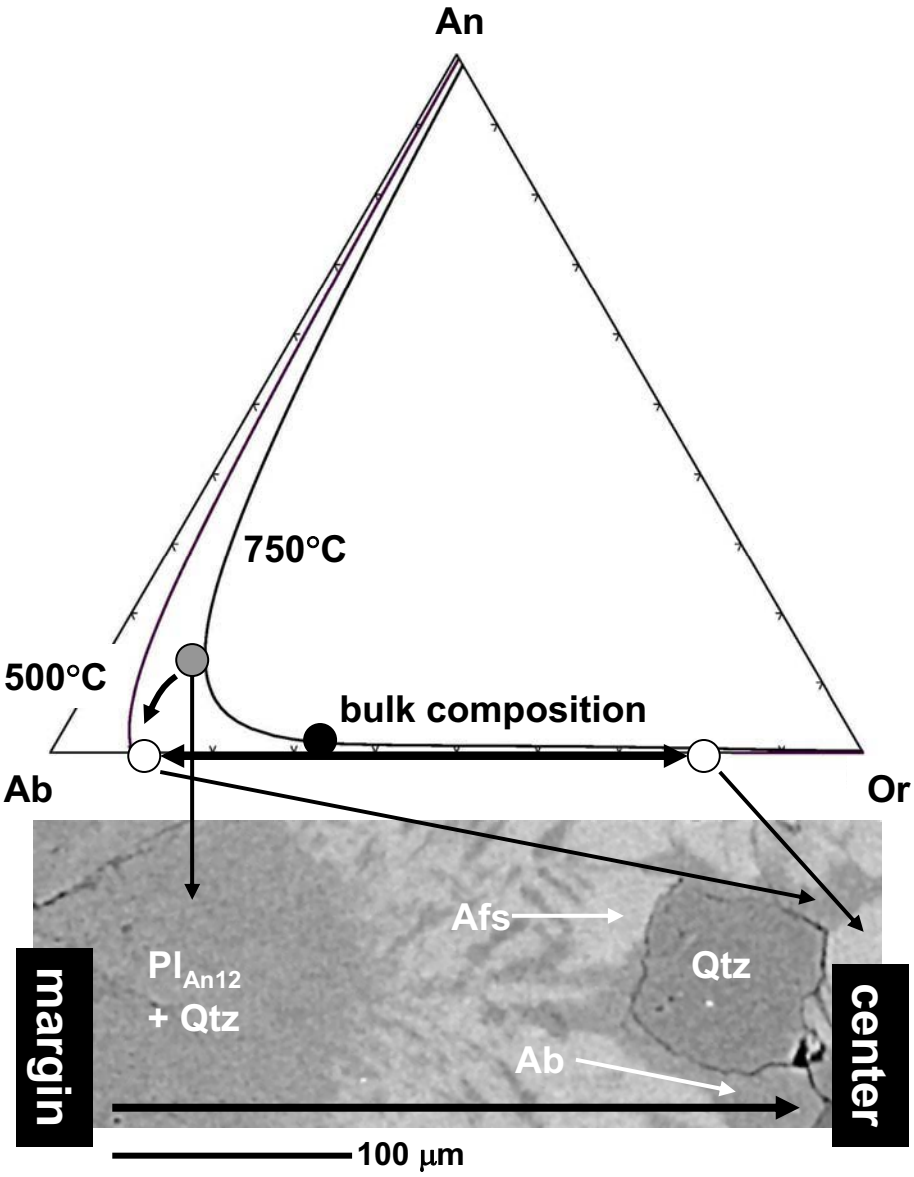
An
750°C
500°C
bulk composition
Ab
Or
Afs
Qtz
Pl_{An12}
+ Qtz
Ab
margin
center
100 μm

Fig 3

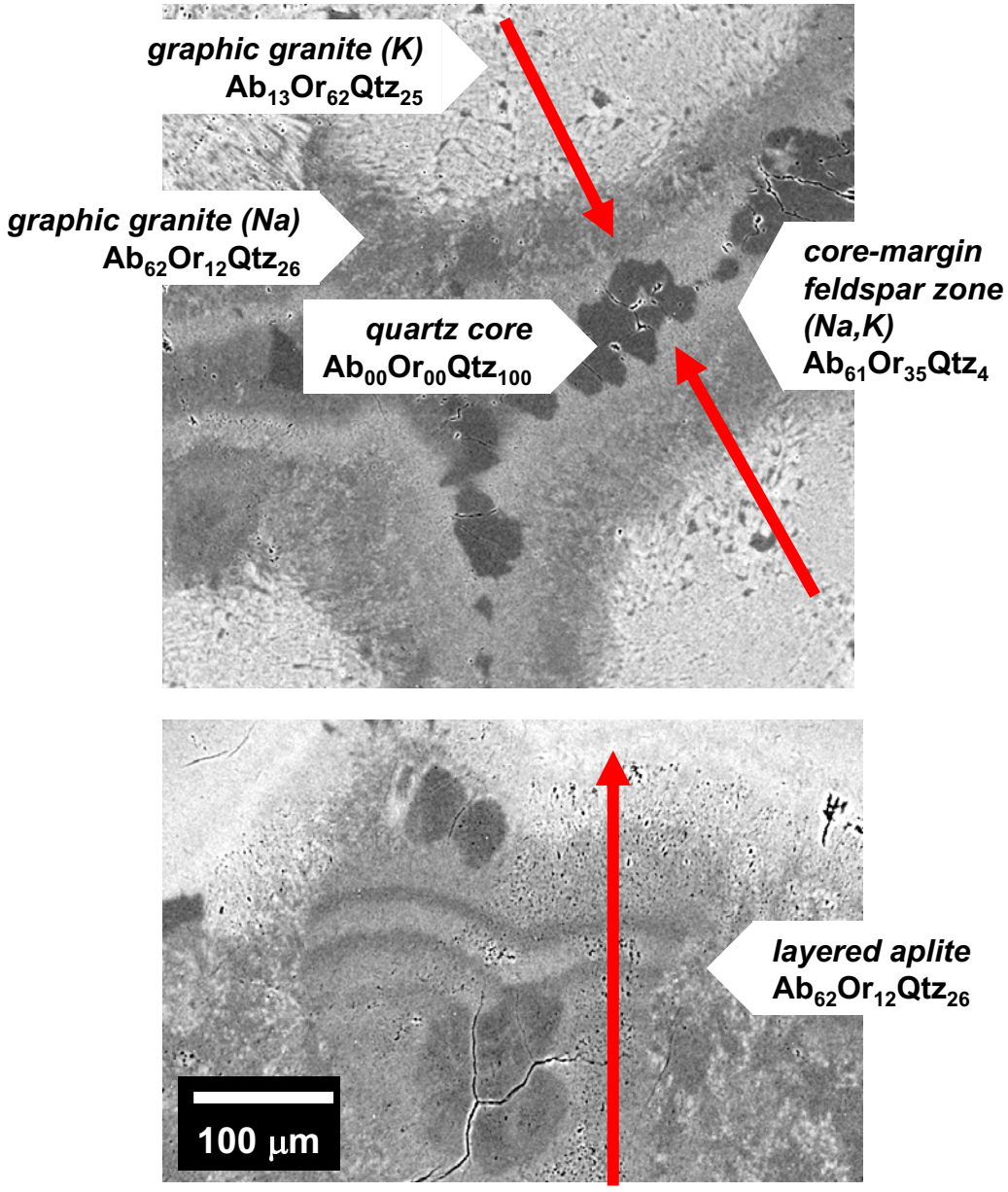
graphic granite (K)
$Ab_{13}Or_{62}Qtz_{25}$
graphic granite (Na)
$Ab_{62}Or_{12}Qtz_{26}$
quartz core
$Ab_{00}Or_{00}Qtz_{100}$
core-margin feldspar zone (Na,K)
$Ab_{61}Or_{35}Qtz_4$
layered aplite
$Ab_{62}Or_{12}Qtz_{26}$
100 µm